Biomaterials 53 (2015) 239–250

Contents lists available at ScienceDirect

Biomaterials

journal homepage: www.elsevier.com/locate/biomaterials

Nanoparticle delivery of stable miR-199a-5p agomir improves the osteogenesis of human mesenchymal stem cells via the HIF1a pathway

Xiao Chen [a, b, 1], Shen Gu [b, 1], Bi-Feng Chen [b, c], Wei-Liang Shen [a], Zi Yin [a], Guo-Wei Xu [a], Jia-Jie Hu [a], Ting Zhu [a], Gang Li [b], Chao Wan [b], Hong-Wei Ouyang [a], Tin-Lap Lee [b, **], Wai-Yee Chan [b, *]

[a] Zhejiang Provincial Key Laboratory of Tissue Engineering and Regenerative Medicine, Zhejiang University, Hangzhou, Zhejiang Province, China
[b] School of Biomedical Sciences, The Chinese University of Hong Kong, Hong Kong Special Administrative Region
[c] Department of Bioscience and Biotechnology, School of Chemical Engineering and Life Sciences, Wuhan University of Technology, Wuhan, China

ARTICLE INFO

Article history:
Received 26 October 2014
Received in revised form
10 February 2015
Accepted 15 February 2015
Available online

Keywords:
Human mesenchymal stem cells
hsa-mir-199a
Drug delivery
Bone differentiation
Maturation
Regeneration

ABSTRACT

Elucidating the regulatory mechanisms of osteogenesis of human mesenchymal stem cell (hMSC) is important for the development of cell therapies for bone loss and regeneration. Here we showed that hsa-miR-199a-5p modulated osteogenic differentiation of hMSCs at both early and late stages through HIF1a pathway. hsa-miR-199a expression was up-regulated during osteogenesis for both of two mature forms, miR-199a-5p and -3p. Over-expression of miR-199a-5p but not -3p enhanced differentiation of hMSCs *in vitro*, whereas inhibition of miR-199a-5p reduced the expression of osteoblast-specific genes, alkaline phosphatase (ALP) activity, and mineralization. Furthermore, over-expression of miR-199a enhanced ectopic bone formation *in vivo*. Chitosan nanoparticles were used for delivery of stable modified hsa-miR-199a-5p (agomir) both *in vitro* and *in vivo*, as a proof-of-concept for stable agomir delivery on bone regeneration. The hsa-mir199a-5p agomir were mixed with Chitosan nanoparticles to form nanoparticle/hsa-mir199a-5p agomir plasmid (nanoparticle/agomir) complexes, and nanoparticle/agomir complexes could improve the *in vivo* regeneration of bone. Further mechanism studies revealed that hypoxia enhanced osteogenesis at early stage and inhibited osteogenesis maturation at late stage through HIF1a-Twist1 pathway. At early stage of differentiation, hypoxia induced HIF1a-Twist1 pathway to enhance osteogenesis by up-regulating miR-199a-5p, while at late stage of differentiation, miR-199a-5p enhanced osteogenesis maturation by inhibiting HIF1α-Twist1 pathway.

1. Introduction

Human mesenchymal stem cells (hMSCs) are a population of self-renewing multipotent cells that can be derived from various tissues, including bone marrow, adipose tissue, blood, cord, pulp, and periodontal ligaments. They are progenitor cells capable of differentiating into a variety of mature tissues. They also have significant clinical potential in cell therapies for tissue regeneration [1–8]. hMSCs readily undergo osteoblastic differentiation when exposed to osteogenic induction media. Therefore they are good noncancerous models for studying osteogenic differentiation and bone regeneration. MSC differentiation involves complex pathways that are regulated at both transcriptional and posttranscriptional levels.

miRNAs play a significant role in human MSC differentiation. In human, disruption of the Dicer gene, which is critical for mature miRNAs formation, resulted in interruption of MSC differentiation [9]. Previous studies in mouse showed more than 10-fold up-regulation of miR-199a during chondrogenesis [10]. However, miR-199a-3p was shown to be a negative regulator in early chondrogenesis in mouse [11], indicating that the functions of miR-199a on differentiation could be stage-specific. In addition, the gene *Dnm3os* which encodes the miR-199a-2/214 cluster was shown to

* Corresponding author. Tel.: +852 3943 1383; fax: +852 2603 7902.
** Corresponding author.
E-mail addresses: leetl@cuhk.edu.hk (T.-L. Lee), chanwy@cuhk.edu.hk (W.-Y. Chan).
[1] These authors contributed equally to this work.

http://dx.doi.org/10.1016/j.biomaterials.2015.02.071
0142-9612/

be indispensable for normal growth and skeletal development in mouse [12]. In human, previous work showed that miR-199a-5p was highly expressed in human MSC during osteo-chondro lineage differentiation [9,13]. However, the functions of miR-199a in stem cell differentiation are not clear.

Since gene therapy approach could prolong the availability of therapeutic proteins, it is considered to be a promising method for inducing *in vivo* regeneration [14]. Gene therapy for delivering synthesized microRNA (miRNA) to modulate the level of gene expression offers ideal therapeutic potentials for a variety of pathologic conditions. Thus, various vectors employed in DNA delivery have been developed to enhance gene delivery, such as viral vectors, liposomes, and other delivery systems. Viral vectors are widely used because of their high transfection efficiency. However, the disadvantages, including toxicity, cellular immune response and oncogenicity due to insertional mutagenesis, etc, limited their application in gene delivery. Non-viral methods have been paid more attentions to because of ease of synthesis, low immune response, high biocompatibility and safety [8,15–18]. However, limitations to topical delivery for regenerative applications including that for miRNA are relatively short half-life, especially in rapidly dividing cells (i.e., in regenerating tissue), poor cellular uptake, rapid degradation by nucleases, and limited blood stability [19]. As a result of these limitations, success of unassisted delivery of miRNA to the cells and tissues is disappointing. Agomirs are chemically modified miRNAs which can be used to overcome these problems. The modifications posses advantages such as increased serum stability, improved cellular uptake and increased stability in cells. These advantages made the agomirs popular for *in vivo* applications. Current *in vivo* delivery method of agomir is direct injection into the blood or tissues. Injection has to be done at least twice a week and high dose injection of agomir may cause side effects, which hindered the *in vivo* application of the agomir. Therefore, biodegradable systems which can transport agomirs for regenerative medicine with controlled and sustained miRNA delivery *in vitro* (i.e., ranging 20–50 days of release *in vitro*) are needed. Scaffolds that promote new tissue in-growth are also needed to exploit the promising potential offered by successful delivery of agomir.

Nanoparticle, as a non-viral vector with biodegradability and controlled release ability, has been used frequently in gene transfer. It can combine and concentrate DNA and RNA and effectively introduces the combined or concentrated product into a variety of cells. Due to their nano-size range, polymeric nanoparticles containing genes could overcome the absorption barrier of the cell membrane by penetrating the cell via endocytosis [20,21]. In recent years, chitosan-based carriers are one of the non-viral vectors that have gained increasing interest as a safer and cost-effective delivery system for genetic materials including plasmid DNA, siRNA, mature miRNA, pre-miRNA, as well as proteins and peptides. Chitosan has beneficial qualities such as low toxicity, low immunogenicity, excellent biodegradability, and biocompatibility [22]. Chitosan has the polymeric backbone with high positive charge and can form nanosize complexes with oppositely charged nucleic acids, including siRNA and miRNA. It can enhance their cellular uptake by binding to negatively charged cellular membranes and protect the miRNA from being digested by endogenous nucleases [23]. However little is known about the usefulness of chitosan nanoparticle for agomir delivery in the treatment of injuries *in vitro* and *in vivo*. In this study, we reported that miR-199a could enhance osteogenesis of hMSC and agomirs loaded into chitosan hydrochloride nanoparticles and could improve bone repair. The characteristics of the nanoparticle/agomir complexes, transfection efficiency, and efficiency of injured bone repair with the nanoparticle/agomir complexes were evaluated.

In addition, we identified the key mechanism with which miR-199a regulates osteogenesis of hMSCs. hsa-miR-199a-3p and -5p are two matural forms of the same miR-199a precursor. They have been shown to exhibit a wide spectrum of activities in various types of tissues and disease models [24]. In this study, we investigated the roles of miR-199a in hMSCs, focusing on its different functions at different stages during hMSC differentiation. We hypothesize that miR-199a-5p improves MSC differentiation via a HIF1α-Twist1 pathway. We identified miR-199a-5p as a potential promoter during osteoblast differentiation and enhancer of regeneration potential of hMSCs. By modulating miR-199a-5p activity, we showed that miR-199a markedly increased osteogenic differentiation *in vitro* and enhanced ectopic bone formation *in vivo*, whereas inhibition of miR-199a-5p reversed these effects. The inhibitory effect of miR-199a-5p on its direct target HIF1α has been well established in cardiomyocytes and various types of cancer cells [25–27]. We investigated the HIF1α-Twist1 pathway during differentiation of human MSCs. The expression of miR-199a is controlled by a HIF1α and Twist1 cyclic pathway via an E-Box promoter element and could promote the initiation of differentiation at an early stage. In addition, miR-199a-5p at maturation stage inhibited HIF1α and Twist1 cyclic pathway. Our findings demonstrated that HIF1α-Twist1-miR-199a cyclic pathway could regulate MSC osteogenesis and the regulation mechanisms are different at different differentiation stages.

2. Materials and methods

2.1. Isolation and expansion of MSCs

The present study was approved by the Clinical Ethics Committee of The Chinese University of Hong Kong. Umbilical cords were obtained from consenting patients delivering full-term infants. Cord MSC (Wharton's jelly-derived MSC) were derived as described previously [28]. Briefly, cords were collected in sterile PBS solution and immediately transferred to the laboratory for cell isolation. Cords were cut into pieces of 3–4 cm, and sections were incised along their length to expose underlying Wharton's jelly. The umbilical vein and the 2 arteries were pulled away, and the remaining mesenchymal tissues were cut into 1 mm^3 and centrifuged at 250g for 5 min at room temperature.

The pellet was suspended in F12/MEM (Life technologies, Merelbeke, Belgium) supplemented with 1 mg/mL collagenase type I, hyaluronidase (Sigma, Aldrich Inc., St. Louis, MO, USA)), 100 U/mL penicillin, and 100 ug/mL streptomycin (Invitrogen) and transferred to a 10 cm dish (Corning). Tissues were digested at 37°C and 5% CO_2 atmosphere for 18–24 h. The homogenate was diluted in Dulbecco's phosphate-buffered saline (Invitrogen) and centrifuged at 600g for 15 min. The cell pellet was re-suspended in expansion medium composed of F12/MEM medium supplemented with 15% fetal bovine serum (Invitrogen), 100 U/mL penicillin, and 100 ug/mL streptomycin (Invitrogen). Viable cells were counted using trypan blue exclusion assay. Cells were seeded in a single 75 cm^2 tissue culture flask at a density of 10^4 cells/cm^2. Plated cells were cultured in expansion medium at 37°C and 5% CO_2 in a fully humidified atmosphere. At 80%–90% of confluence, cells were detached from the flask using 0.05% trypsin/EDTA solution (Invitrogen). Cells were replated at a density of 10^4 cells/cm^2 in expansion medium, and medium was changed every 3 days. Cells were used for differentiation and regeneration at passage 3 to 4.

2.2. Multipotent differentiation

We studied the *in vitro* multi-differentiation potential of the umbilical cord-derived MSCs (UCMSCs) toward osteogenesis, adipogenesis, and chondrogenesis as described previously [29]. For osteogenic differentiation of UCMSCs, cells at passage 3 were plated at a density of 5×10^3 cells/cm^2 and induced under HG-DMEM with 0.02 M β-glycerol phosphate, 10 nM dexamethasone, and 50 ug/ml ascorbic acid. Chondrogenic differentiation was induced in mass cultures with TGF-β1. Adipogenic differentiation was induced in expanded UCMSCs, and cultured by treatment with 1-methyl-3-isobutylxanthine, dexamethasone, insulin, and indomethacin. Positive adipogenic induction was detected by oil red staining for lipid vacuoles.

2.3. Alkaline phosphatase (ALP) and alizarin red staining (ARS)

ALP activity was assayed using a BCIP/NBT alkaline phosphatase color development kit (Beyotime Institute of Biotechnology). DAPI (Beyotime Institute of Biotechnology) was used to stain nuclei. ALP-positive cells were counted under a light microscope (Olympus IX71) in five randomly selected fields. For quantification of alkaline phosphatase (ALP) activity, the SensoLyte® pNPP Alkaline Phosphatase

Assay Kit (Anaspec) was used following the manufacturer's protocol. Calcium deposits were detected by staining with 2% alizarin red S (pH 4.2; Sigma). To quantify the stained nodules, the stain was solubilized with 0.5 ml 5% SDS in 0.5 N HCl for 30 min at room temperature. Solubilized stain (150uL) was transferred to wells of a 96-well plate, and absorbance was measured at 450 nm. Data are presented as means ($n = 4$).

2.4. Cell viability and proliferation assay

Cell viability and proliferation were measured with a Cell Counting KIT-8 (CCK-8, Dojindo). The hMSC at desired time points, were incubated in CCK-8 solution in a 5% CO_2 incubator at 37°C for 2 h. The intense orange-colored formazan derivative formed by cell metabolism is soluble in the culture medium. The absorbance was measured at 450 nm with a reference wavelength of 650 nm. Cell number was correlated to optical density (OD).

2.5. Chitosan nanoparticles/agomir preparation

Chitosan hydrochloride with molecular weight of 110 kDa (Cl113) (Ultrapure, Aoxing Bio, Zhejiang, China) was used. Pentasodium tripolyphosphate (TPP) was obtained from Sigma–Aldrich. Modified mature miRNA agomir hsa-199a-5p and control agomir with/without cy3 were synthesized by RiboBio Co. Ltd, China). Chitosan hydrochloride was dissolved in distilled water to form different concentrations of chitosan solution, ranging from 25 to 300 ug/ml. Nanoparticles were produced based on modified ionic gelation of tripolyphosphate (TPP) with chitosan as described elsewhere [30]. Nanoparticles were spontaneously obtained upon the addition of 1.2 ml of a TPP aqueous solution (0.84 mg/ml) to 3 ml of chitosan solution (2 mg/ml, at chitosan to TPP weight ratio of 6:1) under constant magnetic stirring at room temperature. The particles were then incubated at room temperature for 30 min before use or further analysis. Nanoparticles were collected by centrifugation (Eppendorf) at 13,000 × g for 10 min. The supernatants were discarded and nanoparticles were resuspended in distilled water. The chitosan and agomir ratio of the nanoparticle/miRNA complexes were determined as described previously [30]. For the association of agomir with the chitosan–TPP nanoparticles (nanoparticles/agomir), 3 ul of agomir (19.95 ug/ul) with/without 3 ul Lipofectamine 2000 in double distilled water was added to the TPP solution (1.2 ml, 0.84 mg/ml) before adding this drop-wise to the chitosan solution (3 ml, 2 mg/ml) under constant stirring at room temperature. The particles were then incubated at room temperature for 30 min before use or further analysis and rat tibia defect regeneration.

2.6. Determination of agomir loading efficiency

The loading efficiency of agomir entrapped or adsorbed onto the chitosan nanoparticles was obtained from the determination of free agomir concentration in the supernatant recovered after particle centrifugation (13,000 × g, 15 min) by absorbance measurement at 260 nm or by using qPCR of miRNA. Supernatant recovered from unloaded chitosan–TPP nanoparticles (without agomir) was used as a blank. Agomir loading efficiency (%) was the percentage of entrapped agomir to the total amount of miRNA-agomir added.

2.7. Determination of agomir release efficiency and biological activity of nanoparticles/agomir

Nanoparticles/agomirs (10 ul) were suspended in pH 7.2 PBS (1 ml) and culture media (DMEM, 10%FBS) buffer solutions (1 ml). The suspensions were kept at 37C under gentle shaking. At specific time points, the suspensions (100 ul) were centrifuged at 10,000 × g for 2 min to remove unhydrolyzed particles. The supernatant (6 ul) was subjected to cDNA synthesis followed by conversion to miRNA using a qRT-PCR Kit (Invitrogen, Carlsbad, CA). The amount of miRNA released from the nanoparticles was measured using a FAST 7900 Real-Time PCR system (Life Technologies, Grand Island, NY).

In vitro transfection studies were performed in hMSC cells. The cells were seeded in a 12- well plate at a density of 60,000 cells per well in DMEM containing 10% of FBS without antibiotics, 24 h prior to transfection. On the day of transfection, supernatant of released agomir were add to the cultured media. After incubation at 37 °C with a 5% CO_2 atmosphere for 6 h, the medium was removed and the cells were washed with PBS. The medium was replaced with 1000 ul fresh medium containing serum. After 48 h, the expression level was determined by qPCR.

2.8. RNA isolation, RT-PCR, and quantitative real-time PCR (qPCR)

Total cellular RNA was isolated by lysis in TRIZOL (Invitrogen) followed by one-step phenol/chloroform/isoamyl alcohol extraction as described in the protocol of the manufacturer. 500 ng of total RNA was reverse-transcribed into cDNA by incubation with 200 U of reverse transcriptase in 10 ul of reaction buffer at 37°C for 1 h using Takara RT kit (Takara, Bio Inc., Shiga, Japan)). One microliter of cDNA was used as a template for the qPCR. All gene transcripts were quantified by quantitative PCR with Brilliant SYBR Green QPCR Master Mix (ABI) and a Light Cycler (ABI 7900HT). For miRNA quantification, qRT-PCR primers specific for human miR-199a and internal control U6 were purchased from Applied Biosystems. The level of expression of each target gene was then calculated as $-2^{\Delta\Delta Ct}$.

2.9. Transfection of miRNA for differentiation

miRNA inhibitor and miRNA mimics were purchased from GenePharma Company (Shanghai, China). Transfections of 25 nM miRNA mimics or 50 nM miRNA inhibitor with lipofectamine 2000 (Invitrogen) were performed according to the manufacturer's instructions in opti-MEM Reduced Serum(Invitrogen). For early stage functional studies of miRNA on osteogenesis, MSCs were transfected before induction. For late stage functional studies, MSCs were transfected at day 5 of differentiation.

2.10. Luciferase reporter assay for miR-199a-2 promoter activation

The flanking sequence from promoter of miR-199a-2 containing the E-box binding site of Twist1 was cloned into the pGL3 luciferase reporter vector (Promega). The plasmid was co-transfected with Twist1 expression vector (pcDNA-Twist1 vector, a gift from Dr. Thomas G. Boyer) into MSC. *Renilla* luciferase plasmid (pGL 4.73, Promega) was used as luciferase activity control. 48 h after transfection, cells were lysed and luciferase activity was measured by GloMax 20/20 Luminometer (Promega) using the Dual-Luciferase Reporter Assay System Kit (Promega).

2.11. Immunofluorescence

Cells were cultured under induction. Runx2, collagen I and osteocalcin were detected using confocal microscopy (BX61W1-FV1000). Briefly, cells were fixed in 4% ($v.v^{-1}$) paraformaldehyde for 10 min at room temperature, permeabilized, and blocked for 30 min with 0.1% Triton X-100 and 1% bovine serum albumin. Fixed cells were washed and incubated for 1 h with an antibody against Runx2 (Sigma), Collagen I (Abcam Inc.), Osteocalcin (Millipore), or control IgG. Cells were incubated with Fluorescence-conjugated secondary antibody (Invitrogen) for 30 min and observed under a confocal microscopy. Nuclei were stained with DAPI.

2.12. Ectopic in vivo bone formation assay of transfected hMSC cells

hMSCs were transfected as described above, loaded on hydroxyapatite/collagen (HA/collagen), and implanted s.c. into 8-wk-old NOD. Briefly, cells (5×10^5) were resuspended in 50 uL medium, seed to wet HA/collagen, incubated at 37 °C for 2 weeks of induction, and then implanted in NOD/SCID mice. Engineered bones were divided into 5 groups, including normal induction, miR-199a-5p group, hypoxia, short stage hypoxia and hypoxia with miR-199a-5p group (four duplicates) (see Fig. 6A). Each mouse received two identical implants (one on each side). Implants were removed after 6 weeks; samples were detected by X-ray detection, fixed in 4% paraformaldehyde and decalcified in formic acid for HE staining.

2.13. Rat tibia defect animal model

The animal research protocol was reviewed and approved by the animal center committee of Zhejiang University. The tibia bone defects were created in 8-week-old Sprague–Dawley (SD) Rat under general anesthesia using xylazine and ketamine. Before the operation nanoparticle/agomir containing 0.5 nmol agomir were resuspended in 20 ul fibrin gel for implantation. The animals were placed on a heating pad for maintenance of body temperature. After shaving the hind limb, the diaphysis of (left or right) tibia was exposed by longitudinal skin incision on the medial aspect of hind limb. Defect diameter of 3 mm in both of tibia bones was generated using a hand drill trephine burr with constant saline irrigation. In the experimental limbs, bone defects were treated with nanoparticles/199a-5p agomir in 20 ul fibrin gel, whereas the control limbs were treated with nanoparticles/199a-5p agomir in 20 ul fibrin gel. The skin was then resealed. The procedure was performed under sterile conditions. Animals were at 8 weeks after implantation for radiographic and histological analysis.

2.14. Histological examination

Specimens were immediately fixed in 10% neutral buffered formalin, dehydrated through an alcohol gradient, cleared, and embedded in paraffin blocks. Histological sections (7 um) were prepared using a microtome and subsequently stained with hematoxylin and eosin and Masson trichrome. General histological scoring was performed using hematoxylin and eosin staining.

2.15. Statistical analysis

All data were expressed as mean ± SD, unless otherwise indicated. Statistical comparison between two groups was analyzed by the Student's t-test. For multi-groups, data was analyzed using analysis-of-variance (ANOVA) to determine the presence of any significant difference between groups, followed by LSD (least significant difference) test to determine the values that were significantly different. P-values of 0.05 were deemed to be statistically significant.

3. Results

3.1. hsa-miR-199a up-regulation during MSC osteogenesis and miR-199a-5p, but not -3p induced differentiation

The morphology and the multi-differentiation potential of hMSC were examined (Fig. S1). After induction of osteogenesis for 14 days, the osteoblast phenotype was confirmed by increased alkaline phosphatase (ALP) activity, Alizarin red staining (ARS) for matrix mineralization and increased expression of genes associated with osteoblast differentiation, *ALP* and *SPP1* [31–33] (Fig. 1A). Expression levels of both hsa-miR-199a-5p and hsa-miR-199a-3p were significantly up-regulated during differentiation at day 3 and remained high up to day 14 (Fig. 1B).

To evaluate the biological effects of miR-199a on osteogenesis, inhibition of miR-199a by siRNA and over-expression by miR-199a mimics for both -5p and -3p were performed. Mature miR-199a-5p levels were elevated 400-fold compared to control cells. By comparison, treatment with miR-199a-5p siRNA led to inhibition of miR-199a-5p by 90% (Fig. S2). hMSCs were induced to differentiate

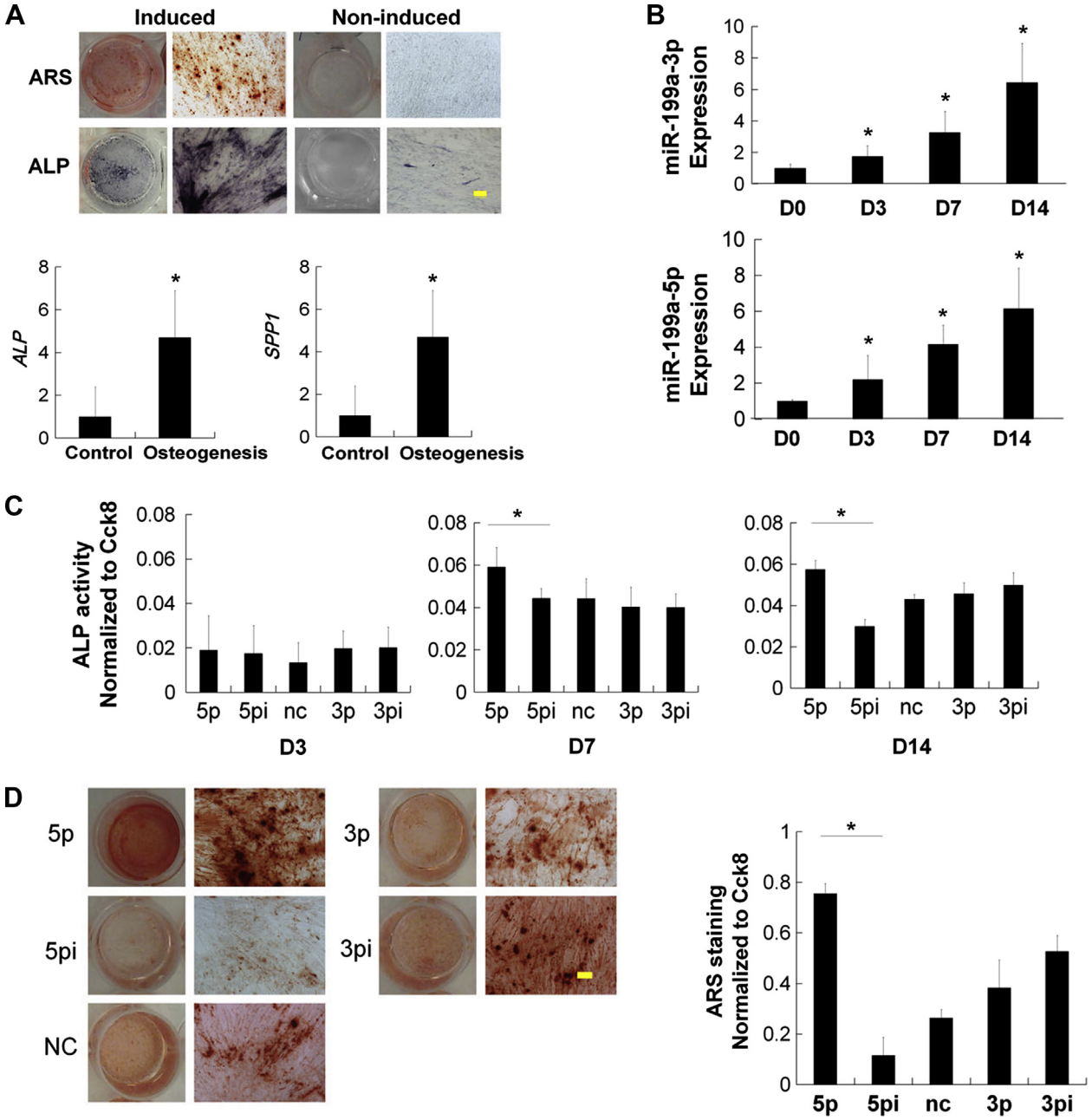

Fig. 1. Osteoblast differentiation and miR-199a-5p, but not -3p induced osteoblast differentiation of hMSC. (A) Alkaline phosphatase (ALP) and Alizarin red staining (ARS) performed at Day 14 of osteogenesis showed that induced MSCs had higher ALP activity and calcium deposition level. Osteoblast differentiation was confirmed by qPCR analysis of osteoblast marker genes (ALP and SPP1 normalized to β-Actin at Day 14 comparing to control). Scale bar = 100um (B) hsa-miR-199a expression was measured after osteogenesis induction at Day 3 (D3), Day 7 (D7) and Day 14 (D14) comparing to undifferentiated MSCs (D0). n = 3 for all experiments.*, $p < 0.05$ compared to control group. (C) To study the effect of miR-199a on osteoblast differentiation, hMSCs transfected with 25 nM scrambled control (NC), hsa-miR-199a-5p (5p), hsa-miR-199a-3p (3p), or hsa-miR-199a-5p siRNA (5pi) and hsa-miR-199a-3p siRNA (3pi) were induced to osteoblast differentiation for up to 14 days. ALP activity was measured at day 3, 7, 14 (D3, D7, D14) of osteoblast differentiation, normalized to cell number (n = 4). (D) ARS were performed at Day 14 and quantification normalized to cell number (n = 3). *, $p < 0.05$. Scale bar = 100um.

toward osteoblasts after transfection with either mature hsa-miR-199a-5p/-3p or hsa-miR-199a-5p/-3p siRNA. Over-expression of hsa-miR-199a-5p significantly enhanced osteoblastic differentiation. This was evidenced by increased ALP activity and enhanced *in vitro* matrix mineralization as visualized by ARS. In contrast, ALP activity and matrix mineralization were reduced in hsa-miR-199a-5p siRNA treated hMSCs. However, we found that neither hsa-miR-199a-3p nor hsa-miR-199a-3p siRNA could change osteoblastic differentiation (Fig. 1C, D). Taken together, these results suggested that miR-199a-5p but not miR-199a-3p was a positive regulator of osteoblast differentiation of hMSCs.

3.2. Characterization of nanoparticles/agomir

The size distributions and the morphology of the chitosan nanoparticles and nanoparticle/agomir complexes were examined by SEM (Fig. 2A–D). The mean diameter of the chitosan nanoparticles and nanoparticle/agomir complexes were about 250 nm, ranging from 0.1 to 0.8 um. However, a smaller mean particle size of chitosan nanoparticles was obtained when fewer agomirs were used compared to the higher concentration of agomirs. Large particles, with sizes bigger than 1000 nm, were obtained when agomirs were add to the chitosan.

To evaluate the compatibility of the nanoparticle/agomir complexes, the *in vitro* cytotoxicity of nanoparticles against human MSC was measured (Fig. 2C). Cell viability was measured by MTT assay after 1 day (D), 3D, 5D, 7D and 10D exposure. It could be seen that the nanoparticle/control–agomir complexes showed no significant cytotoxicity, suggesting that this system is suitable for *in vitro* and *in vivo* applications.

3.3. Release, stability and transfection of agomir in vitro

To test agomir loading efficiency and function, about 82% agomir loading efficiency was measured by spectrophotometry (Fig. 3A) and qPCR for all the entrapped agomir chitosan–TPP nanoparticles. The *in vitro* release and stability of agomir from the nanoparticle/agomir complexes was examined both in culture media and in PBS. Fig. 3B showed the *in vitro* agomir release profile at 37C within the 21 day-monitoring duration. In cultured media, about 30%, 55% and 65% of capsuled agomir was released within 7, 14 and 21 days, respectively (Fig. 3B). Transfection efficiency was investigated via cy3 detection and hsa-miR-199a-5p qPCR. Nanoparticles/agomir released miRNA into the cytoplasm of cells *in vitro* similar to naked agomir (Fig. 3C). During long-term culture, it was observed that the nanoparticle/agomir complexes showed constant expression of

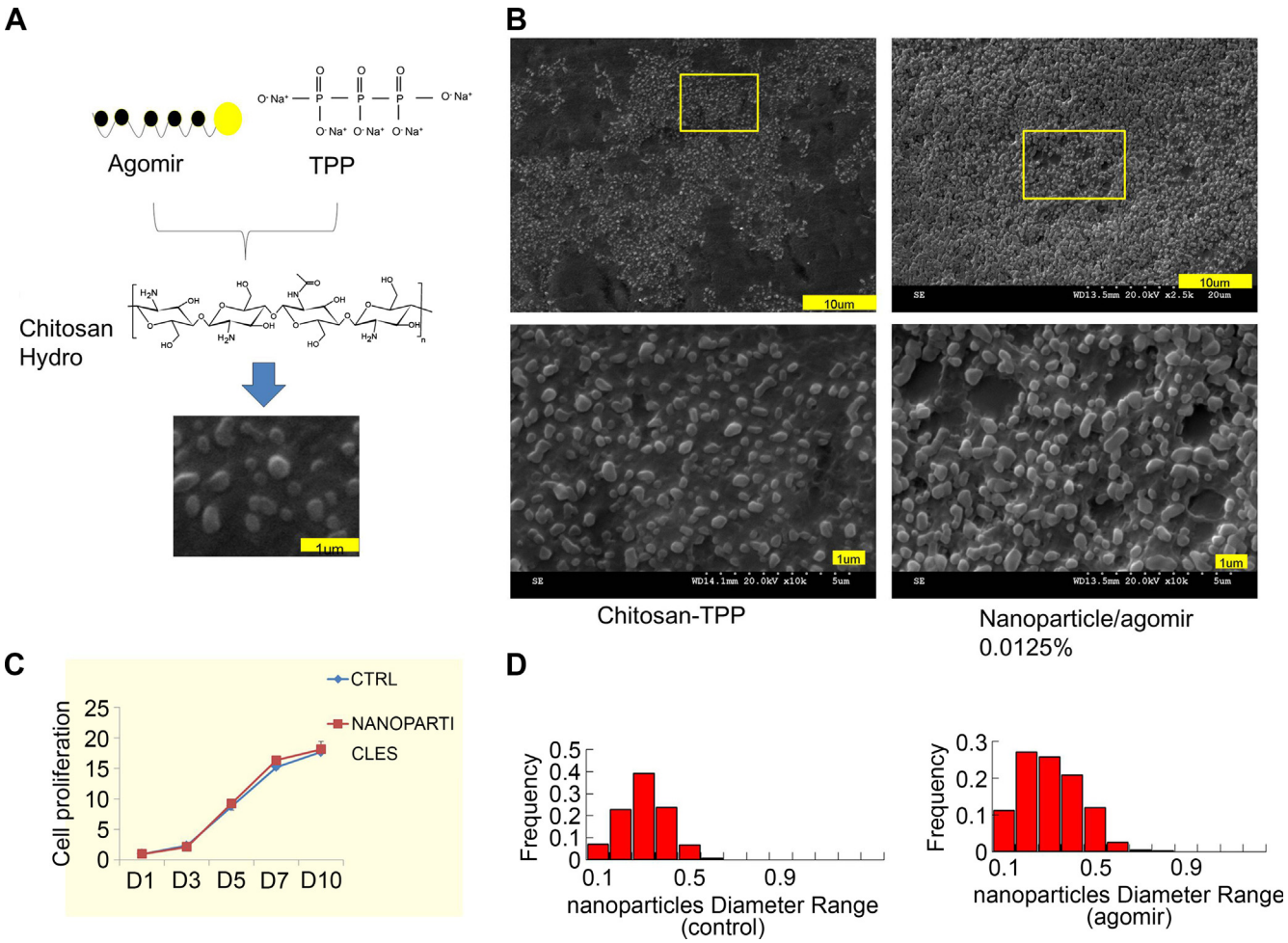

Fig. 2. Preparation and characterization of nanoparticle/agomir. (A) hsa-mir-199a-5p agomir was first complexed with the TPP. Next, the agomir:TPP complexes were added to an chitosan solution, spherical particles of submicron size encapsulating agomir were generated as shown by the scanning electron micrograph. (B) the SEM of the nanoparticles/agomir. (C) *in vitro* Toxicity the nanoparticles/agomir. Viability of human MSCs incubation with the nanoparticles/agomir extract. (D) The nanoparticle size distribution calculated from electron micrograph images shows the mean diameters of nanoparticles/agomir ranging from 0.1 to 0.8 um. Scale bar = 10 um, 1um.

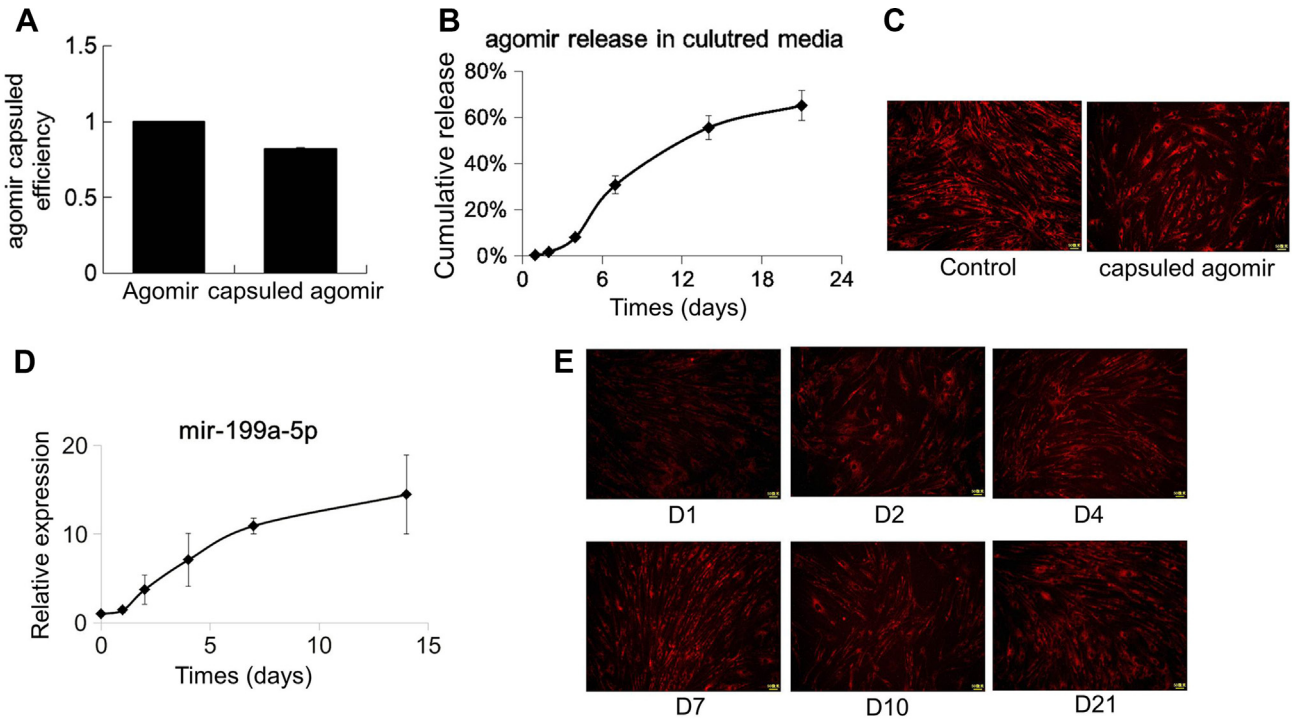

Fig. 3. Release and transfection of agomir *in vitro*. (A) The efficiency of the agomir encapsuled in nanoparticles (n = 3) measured by spectrophotometry. (B) Release nanoparticles/agomir in PBS and FBS. Released miRNAs were measured by qRT-PCR of miR-199a-5p at indicated time points. (C) Nanoparticles/agomir released miRNA into the cytoplasm of cells *in vitro* similar to freshly Agomir. n = 3, means±SD (D) Transfection efficiency of nanoparticles/agomir complexes determined in hMSCs. (E) Typical fluorescent field images of Cy3 in hMSC treated after a period of times. Scale bar = 50 um.

miRNA and the naked agomir had no fluorescence after ten days (Fig. 3E). In order to quantify transfection efficiency and over-expression of miRNA in cells, hMSCs were transfected with miRNA released at different period in the cellular assay. After 48 h, qPCR was used to quantitate the expression level of hsa-mir-199a-5p. Transfection efficiencies were compared. The results corroborated with the outcome of the fluorescence images and indicated that this effective control-release system could be used for the delivery of agomir in regenerative medicine.

3.4. Involvement of HIF1α, Twist1 and miR-199a-5p during osteogenesis of hMSC at early stage and late stage of differentiation

To understand the role of hsa-miR-199a-5p in osteogenesis, we searched for targets of miR-199a-5p with a potential role in osteoblast differentiation. hsa-miR-199a-5p was predicted to target HIF1α, which is the main factor induced by hypoxia and together with Twist1, comprise the key negative regulators of osteogenic differentiation in cultured MSC [34]. However, HIF1α and Twist1 are also essential for early stage bone development and regeneration [35], indicating that HIF1α-Twist1 pathway may play dual roles during osteogenesis at early and late stage.

To investigate how hsa-miR-199a-5p and HIF1α-Twist1 pathway regulate osteogenic differentiation of hMSCs, we treated cells under hypoxia and over-expressed hsa-miR-199a-5p at both early and late stages of osteogenesis. Stages of osteogenic differentiation [36] of hMSC were defined by ALP activity [37] and calcium deposition [38]. We found that after 3 days of induction, ALP activity was low; however, it increased significantly after 5–7 days of induction (Fig. S3). The mineralization level visualized by Alizarin red staining also showed that calcium deposition was formed after 5 days of induction. Therefore 0–5 days of induction was defined as early stage and after 5 days was defined as late stage of osteogenesis.

To investigate the effects of hypoxia on osteogenesis, hMSCs were cultured under hypoxia for 5 days after initiation of induction (early stage) or up to 14 days (late stage). ALP and ARS staining showed that hypoxia at early stage of differentiation could enhance osteogenesis, while hypoxia at late stage of differentiation could inhibit osteogenesis (Fig. S4). To determine whether HIF1α-Twist1 pathway and hsa-miR-199a-5p were involved, the levels of HIF1α and Twist1 in hMSC during osteogenic differentiation were measured by Western blotting. Results showed that HIF1α expression was up-regulated transiently after 2 days of induction, both under normoxic and hypoxic conditions (Fig. S4A). On the other hand, Twist1 protein levels were significantly down-regulated after 5 days under normoxic condition (Fig. S4B), while remained unchanged under hypoxia (Fig. S4A). It indicated that hypoxia may inhibit osteogenesis by maintaining Twist1 protein expression at late stage. Meanwhile, the expression level of hsa-miR-199a-5p was higher under hypoxia condition (Fig. 4B), which was consistent with previous findings that Twist-1 positively regulates the miR-199a/214 cluster during bone development [39]. Therefore, hypoxia may regulate MSC osteogenesis through HIF1α, Twist1 and miR-199a-5p.

3.5. Up-regulation of miR-199a-5p was related to hypoxia enhanced osteogenesis at early stage

As HIF1α and Twist1 are essential during early development of bone, we hypothesized that the HIF1α-Twist1 pathway is essential for early induction of osteogenesis. To determine whether hypoxic condition could increase osteogenesis through HIF1α, Twist1 and hsa-miR-199a-5p at early stage, hMSCs were transfected with HIF1α siRNA, Twist1 siRNA, hsa-miR-199a-5p mimic and hsa-miR-199a-5p inhibitor before induction and the cells were cultured with osteoblast differentiation medium for additional 14 days. Fig. 4 and Fig. S5 showed that both hypoxic condition and hsa-miR-199a-5p

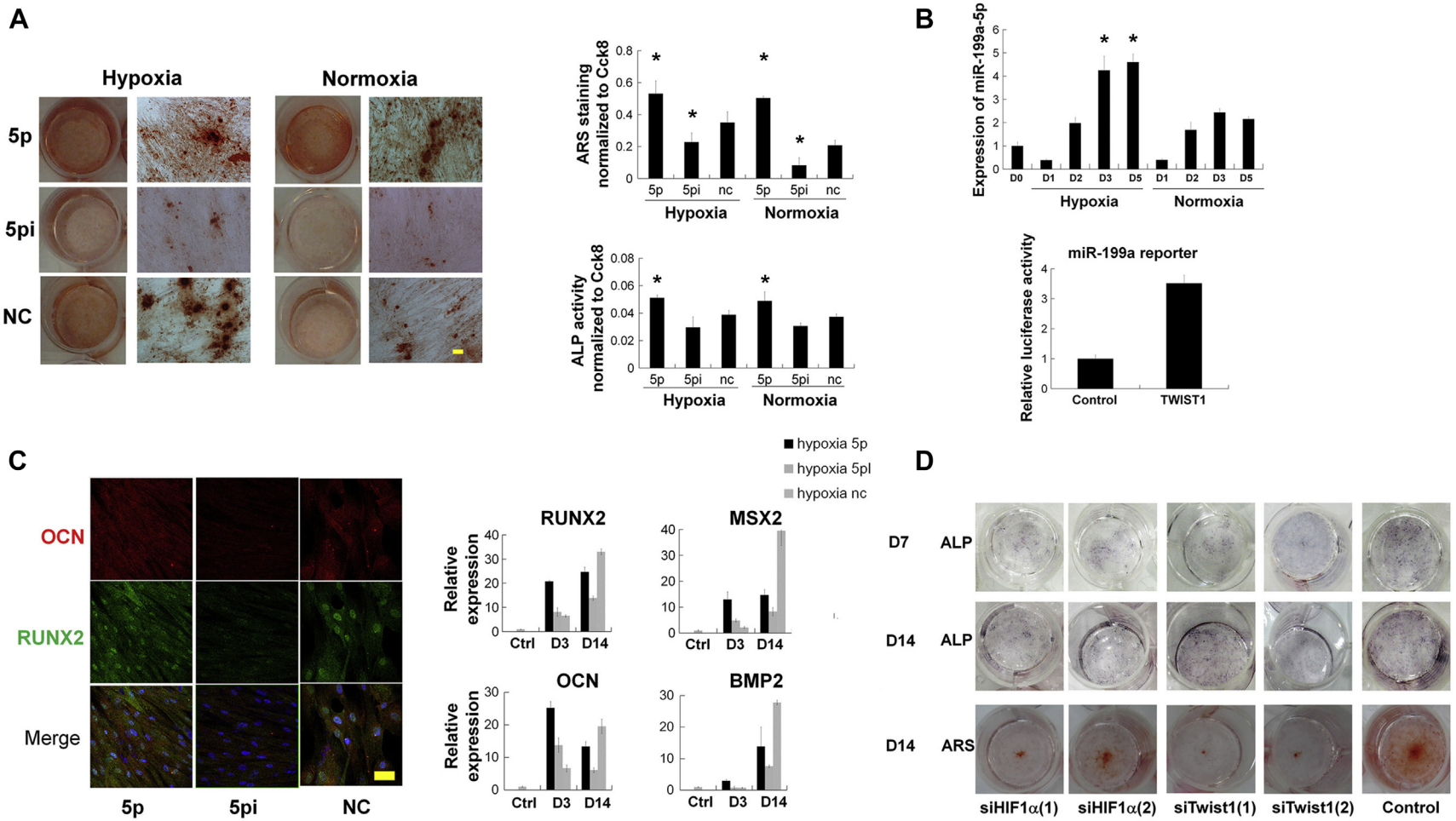

Fig. 4. Hypoxia enhanced osteogenesis at early stage by up-regulating hsa-miR-199a-5p and HIF1a-Twist1-hsa-miR-199a-5p pathway change during osteogenesis. (A) MSCs were treated under hypoxia and/or hsa-miR-199a-5p at early osteogenesis stage. Alizarin Red staining and ALP activity measured at Day 14 showed hypoxia and miR-199a-5p enhanced calcium deposition. Alizarin Red (n = 3) and ALP (n = 4) quantification were normalized to cell number. (B) Hypoxia induced hsa-miR-199a-5p expression during osteogenesis. *, $p < 0.05$ comparing miR-199a-5p expression levels between Hypoxia D3/D5 and Normoxia D3/D5. MSCs were transiently transfected with hsa-miR-199a-2 promoter reporter vector (199a reporter) alone, or with an expression vector encoding Twist1 after 48 h under osteogenesis induction. Luciferase expression levels were normalized to co-transfected *Rentilia* vector (n = 6). (C) Immunostaining of bone specific genes RUNX2 and OCN at day 14 of osteoblast differentiation. qPCR of bone specific genes RUNX2, OCN, MSX2 and BMP2 at Day 3 and 14 of osteoblast differentiation. Scale bar = 20 um. (D) ALP and ARS staining of MSCs transfected with HIF1a siRNA or Twist1 siRNA and then treated with osteoblast differentiation medium for additional 14 days under hypoxia. *, $p < 0.05$ compared to the control.

over-expression at early stage could enhance osteogenesis as evidenced by ARS staining, ALP activity normalized to total cell number and immunostaining of marker genes of bone, RUNX2 and OCN. To further confirm these findings, hMSCs were cultured under hypoxia and/or transfected with hsa-miR-199a 5p at early stage and treated with osteoblast differentiation medium for 3, 7 and 14 days and subjected to qPCR analyses to determine osteogenic marker genes. Early stage hypoxia and miR-199a-5p over-expression significantly increased the expression of bone-related genes, e.g. RUNX2, OCN, MSX2 and BMP2 (Fig. 4 A,C,D and Fig. S5). On the contrary, inhibition of HIF1α, Twist1 and hsa-miR-199a-5p at early stage could reverse the effects under hypoxia (Fig. 4A, D). Our results suggested that hypoxia at the early stage promotes osteogenesis through mir-199 and hsa-miR-199a-5p could play an important role in promoting the osteogenesis potential of hMSCs at early stage of differentiation.

3.6. hsa-miR-199a-5p inhibited HIF1α-Twist1 pathway to increase osteogenesis at late stage

To study the action of miR-199a-5p at late stage of hMSC osteogenic differentiation, hsa-miR-199a-5p mimics were transfected into hMSCs in order to examine whether miR-199a-5p could rescue the osteogenic differentiation potential of hMSCs inhibited by hypoxia at late stage of osteogenesis. hMSCs were transfected with either scrambled miRNA negative control or hsa-miR-199a-5p after 5 days of differentiation induction and treated with osteoblast differentiation medium for additional 9 days. Results showed that hypoxia at late stage could reduce calcium deposition, ALP activity, and expressions of bone specific genes RUNX2 and OCN (Fig. 5A–E and Fig. S6B). However, over-expression of hsa-miR-199a-5p increased ALP activity and mineralized bone matrix formation of hMSCs (Fig. 5A) both under hypoxic and normoxic conditions. To further confirm these findings, hMSCs were treated with hypoxia and/or transfected with hsa-miR-199a-5p at late stage of osteogenesis and treated with osteoblast differentiation medium for 7 and 14 days and subjected to qPCR analysis to determine the expressions of osteogenic marker genes. hsa-miR-199a-5p over-expression significantly increased the expressions of bone related gene RUNX2, SP7, OCN and SPP1 (Fig. 5E and Fig. S6B). These results suggested that hsa-miR-199a-5p could rescue osteogenic differentiation of hMSCs inhibited by hypoxia. To confirm whether hsa-miR-199a-5p rescued osteogenesis at late stage by inhibiting HIF1α-Twist1 pathway, we measured the protein levels of HIF1α and Twist1 at 24 h after transfection with hsa-miR-199a-5p. The results showed that hsa-miR-199a-5p could significantly reduce the level of HIF1α and Twist1. Moreover, inhibition of HIF1α and Twist1 at late stage could reverse the effects of hypoxia (Fig. 5G). Therefore, hsa-miR-199a-5p played an important role in promoting the osteoblast differentiation potential of hMSCs at late stage by repressing the HIF1α-Twist1 pathway.

3.7. hsa-miR-199a-5p and early stage of hypoxia promoted in vivo ectopic bone formation ability

To study whether over-expression of hsa-miR-199a-5p and early stage of hypoxia enhances *in vivo* ectopic bone formation, hMSCs transfected with miR-199a-5p or scrambled control were loaded onto hydroxyapatite-collagen scaffold and implanted subcutaneous in NOD/SCID mice for 6 weeks (Fig. 6A). To address whether the repair was done by tissue engineered bone or radio paque tissue that cannot be distinguished merely by X-ray scanning, both X-ray and histological examination were carried out.

X-ray showed that early stage hypoxia and hsa-miR-199a-5p transfected groups had higher density compared to control group, while late stage hypoxia group showed lower density (Fig. 6B). Histological staining also showed that more bones were formed in the early stage hypoxia and hsa-miR-199a-5p group. Masson trichrome staining for collagen revealed that early stage hypoxia and hsa-miR-199a-5p MSCs after osteogenic induction was stained darker and increased in collagen deposition was found compared with control group (Fig. 6C). In contrast, late stage hypoxia inhibited bone formation and collagen deposition, which could be reversed by hsa-miR-199a-5p transfection. These data suggest that the superior efficiency of early stage hypoxia and hsa-miR-199a-5p on MSCs for bone tissue regeneration.

3.8. Nanoparticle/agomir hsa-miR-199a-5p enhanced in situ regeneration

To evaluate the ability of nanoparticle/agomir in improving the full-thickness bone defect *in vivo*, we surgically induced tibia defects in SD rats and transplanted with nanoparticle/agomir (Fig. 7A). X-ray scanning was first used to evaluate the nanoparticle/agomir in bone formed in the tibia of the experimental model. X-ray scanning showed that more bone-like tissues were formed in the nanoparticle/miR-199a-5p agomir treated group at 8 weeks after implantation. hsa-miR-199a-5p transfected groups had higher density compared to control group (Fig. 7B). H&E staining showed that a few of the nanoparticles still remained around the implantation area after the experiment. No obvious inflammation was found in the repaired cite. H&E and Masson staining revealed more regenerated bone formed in the central part of the repaired area of the nanoparticle/hsa-miR-199a-5p agomir groups (Fig. 7C). Collectively, our results suggested that the nanoparticle/hsa-miR-199a-5p agomir augmented bone regeneration *in vivo*.

4. Discussion

In the present study, we identified hsa-miR-199a as a positive regulator of hMSC osteoblast differentiation and developed a control released system to deliver the stable hsa-miR-199a-5p agomir *in vitro* and *in vivo*. The main findings of our study are: 1) The agomir loaded into chitosan hydrochloride nanoparticles showed stable agomir release for at least 21 days and improved bone repair. 2) *In vitro* experiments revealed that over-expression of hsa-miR-199a-5p enhanced osteoblast differentiation of hMSCs, whereas inhibition of hsa-miR-199a-5p inhibited their osteogenic potential. 3) The function of hsa-miR-199a-5p on osteogenesis was exhibited through regulation of HIF1α-Twist1 pathway. At early stage of osteogenesis, hypoxia enhanced HIF1α-Twist1 pathway to induce hsa-miR-199a-5p expression and promoted osteoblast differentiation. At late stage, high expression of hsa-miR-199a-5p inhibited HIF1α-Twist1 pathway to promote bone maturation. Over-expression of hsa-miR-199a-5p or early stage hypoxia increased ectopic bone formation, whereas late stage of hypoxia significantly diminished bone formation *in vivo*.

Delivery of therapeutic genes and agents to repair tissues can significantly promote cell proliferation and ECM synthesis. Unfortunately, the appropriate vector for miRNA delivery to cells and tissues has not been identified. In our study, we showed that formulated nanoparticles could release their contents over extended periods of time. Chitosan nanoparticle/agomir complexes may be a practical and exciting mode of delivery for promoting miRNA therapy. In this report, we successfully encapsulated the osteogenesis microRNAs agomir into the Chitosan nanoparticle for transfection of cultured hMSCs and promotion of *in vivo* bone regeneration. These particles were made by ion-pairing the agomir. Ion-pairing in this manner was quite efficient and the conjugate was easily extracted to the organic layer for use.

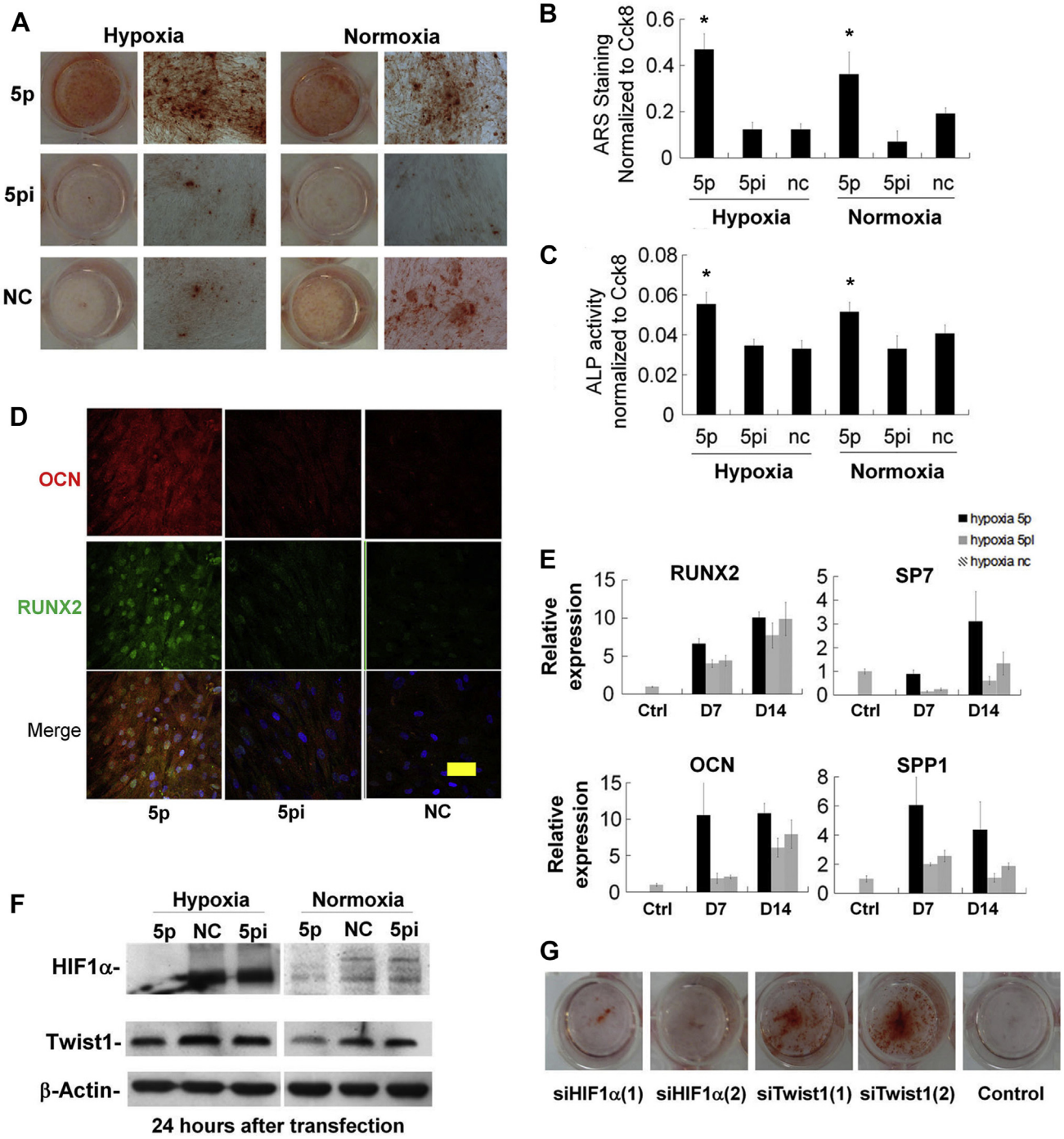

Fig. 5. hsa-miR-199a-5p inhibited hypoxia induced HIF1a-Twist1 pathway to increase osteogenesis at late osteogenic stage. (A) MSCs were treated under hypoxia and/or hsa-miR-199a-5p at late osteogenesis stage after 5 days of induction. Alizarin Red staining performed at day 14 showed that hypoxia reduced and miR-199a-5p enhanced calcium deposition. (B) Alizarin Red quantification normalized to cell number (n = 3). (C) Alkaline phosphatase activity was measured at Day 14 of osteoblast differentiation, normalized to cell number. (n = 4). (D) Immunostaining of bone specific genes RUNX2 and OCN at Day 14 of osteoblast differentiation. (E) qPCR of bone specific genes RUNX2, OCN, SP7 and SPP1 at Day 7 and 14 of osteoblast differentiation. (F) Western blot showed that miR-199a-5p inhibited HIF1a-Twist1 pathway. (G) ARS of MSCs transfected with HIF1a siRNA or Twist1 siRNA at Day 5 and then treated with osteoblast differentiation medium for additional 9 days. *$p < 0.05$ compared to control group. Scale bar = 20um.

Moreover, stem cell differentiation proceeds through defined stages. Understanding the stage specific MSC differentiation condition is crucial for subsequent usage of stem cells in regenerative medicine. The osteogenic differentiation of MSCs is in a tightly regulated manner characterized by cell proliferation, differentiation and production of an extracellular matrix (ECM) composed mainly of type 1 collagen and bone matrix proteins which become progressively mineralized [36]. Recently, hsa-miR-199a-5p was reported to be up-regulated during differentiation of human bone marrow-derived MSCs [9]. These data, together with our findings, suggest a role of hsa-miR-199a-5p in the promotion of hMSC differentiation, at both early and late stage of osteogenesis. Osteoblast

A

Groups	Treatment during tissue engineered bone formation
Control	Normoxia
5p	Normoxia + miR-199a-5p transfection
Early hypoxia	Early osteogenic stage under hypoxia
Late hypoxia	Late osteogenic stage under hypoxia
5p+late hypoxia	Late osteogenic stage under hypoxia + miR-199a-5p transfection

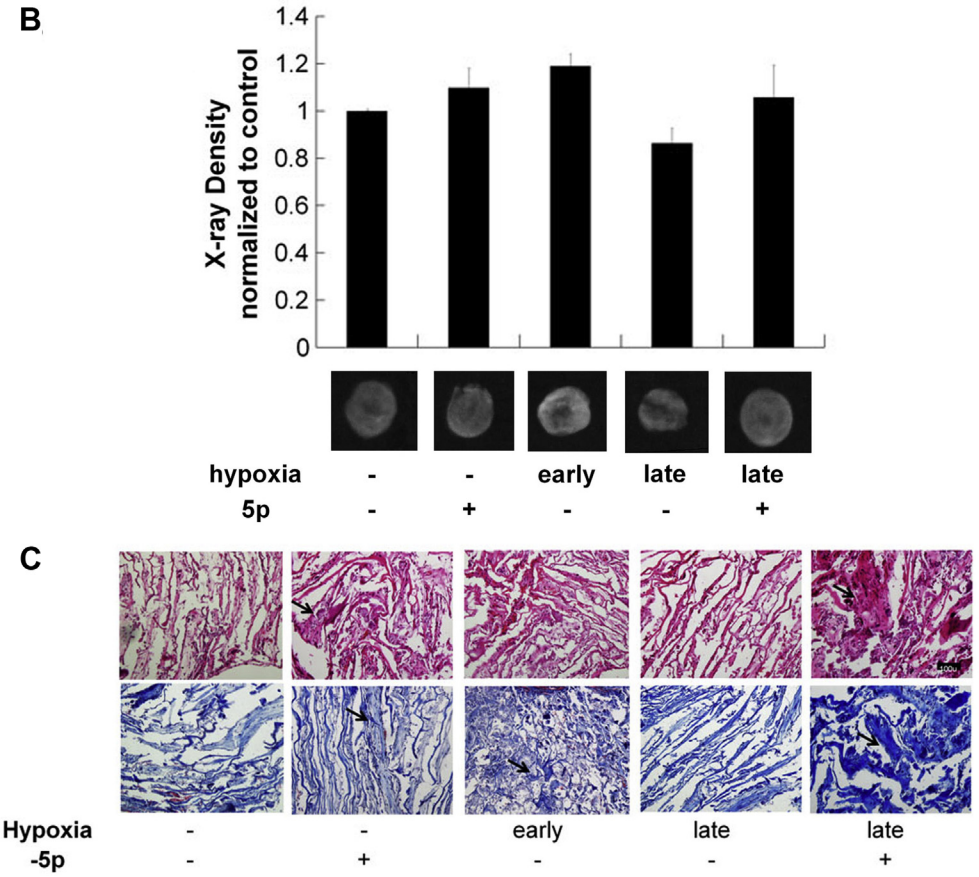

Fig. 6. miR-199a-5p and early stage of hypoxia promoted *in vivo* bone formation. (A) Flow chart depicting *in vivo* bone formation and regeneration. (B) For *in vivo* bone formation, cells were delivered in collagen-ceramic scaffold and induced in osteogenic medium for two weeks followed by transplantation under beneath the dorsal skin of NOD-SCID mice for 6 weeks. Densitometric analysis showed that hsa-miR-199a and early stage of hypoxia promoted *in vivo* bone formation ability. (C) Representative images of Hematoxylin and eosin staining (H&E) for morphologic evaluation and Masson staining for collagen deposition showed that miR-199a-5p and early stage hypoxic cells increased in collagen synthesis. miR-199a-5p could also reverse late stage hypoxia inhibition on osteogenesis. Arrows show the bone formation. Scale bar = 50um.

differentiation can be characterized in three stages: cell proliferation, matrix maturation and mineralization. In our study, early or late stage was divided by ALP activity and calcium deposition *in vitro* [38]. Our data showed that hsa-miR-199a-5p exhibits functions at both early and late stage.

To study the molecular mechanisms by which hsa-miR-199a-5p regulates osteoblast differentiation of hMSC, we searched for potential target genes that have an established function in promoting osteogenesis. Interestingly, HIF1α and its downstream gene target Twist1 had been reported to be key regulators for the proliferation and differentiation of hMSCs [34,40]. HIF1α is a well-established transcription factor that is rapidly induced by hypoxia through a post-transcriptional mechanism in all cell types tested [41]. Most of the studies on HIF1α were conducted in cancer cells. HIF1α, induced during ischemia that occurred in the course of tumor progression or after treatment, stimulates proliferation and induces vascular endothelial growth factor expression and angiogenesis. Hypoxia has also been reported to enhance proliferation, survival, and differentiation of MSCs [40]. Previous study indicated that hypoxia enhanced MSCs to differentiate into osteogenic lineage cells and suggested that Runx2 might be negatively regulated by HIF1α. However, others reported that hypoxia inhibited osteogenesis in MSCs. The detailed mechanism underlying the inhibition effects was unclear [34]. These seemingly controversial findings suggested that MSCs may exhibit a conserved response to reduced oxygen levels and the response on differentiation may be stage dependent. However, little is known about the effect and mechanism of hypoxia on osteoblast differentiation and bone regeneration. Our results showed that hypoxia treatment during early stage of osteogenesis induced higher expression of hsa-miR-199a-5p and

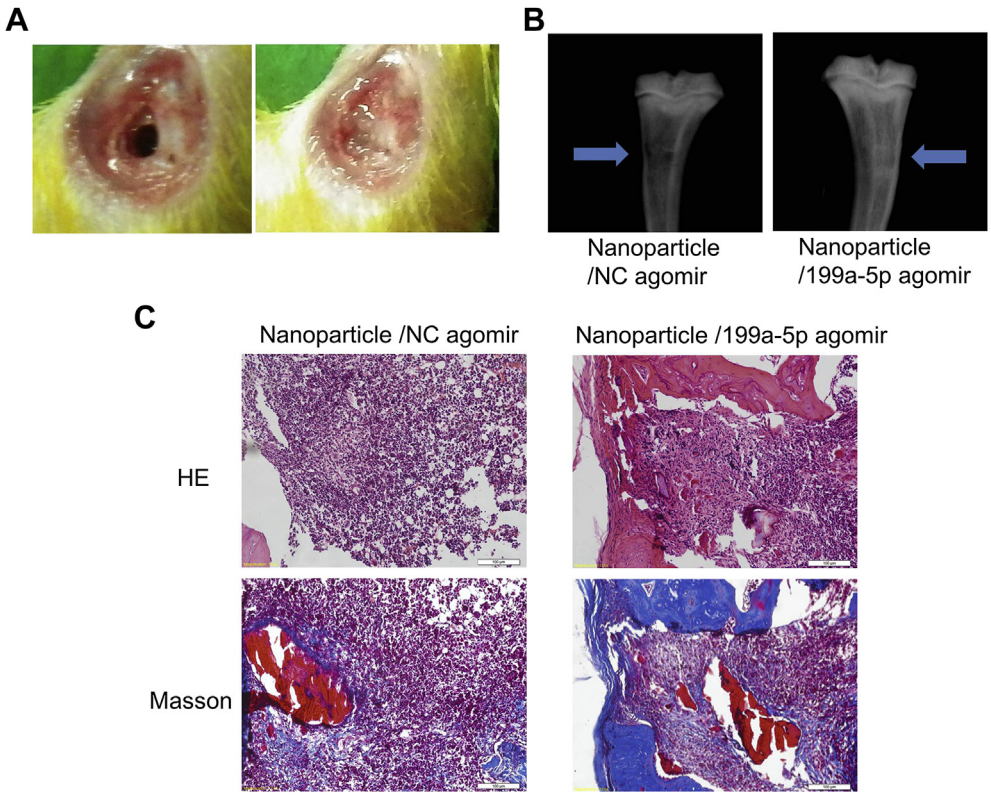

Fig. 7. Nanoparticle/miR-199a-5p agomir enhanced in situ regeneration. (A) A 3 mm round defect was created in the tibia of Sprague–Dawley rats. Nanoparticle/agomir were seeded into a fibrin gel, then the scaffold were placed within the bone defect. (B) Representative X-ray images of the defect, indicating 199a-5p agomir improve new bone formation at the defects. (C) H&E and Masson staining of the repaired bones after 8 weeks of implantation. Arrows indicate the bone formation.

promoted osteogenesis. The functions of HIF1α in MSC differentiation could be different at different differentiation stage and may be mediated by miR-199a-5p.

Twist1 is a basic helix-loop-helix (bHLH) transcription factor which inhibits osteogenesis of MSC [42–44]. During bone development and MSC differentiation, HIF1α and Twist1 proteins interact with Runx2 and inhibit osteoblast differentiation at early stage. However, the function of Twist1 regulating bone development and osteoblast differentiation is not clear [45]. Recently, the HIF1α-Twist1 axis has been found in head and neck cancer and shown to play key roles in tumor metastasis. Since stem cells and cancer cells share a lot of similarities in gene expression, cellular processes and signal transductions, the HIF1α-Twist1 axis could also be involved in the MSC osteogenesis process. Previous studies also showed the direct control of Twist1 on the expression of miR-199a in mouse [12] and human cells [39], and the effect was tissues- and development-stage-specific. Indeed, at early stage of osteogenesis, we found that HIF1α and Twist1 were highly expressed and induced hsa-miR-199a-5p expression, a process important for cellular differentiation. It indicated that HIF1α-Twist1 activation is important for initiation of osteogenesis through up-regulating hsa-miR-199a-5p. While at late stage, we showed that hsa-miR-199a-5p over-expression resulted in down-regulation of HIF1α and Twist1. This strongly suggested that HIF1α-Twist1 pathway is regulated by hsa-miR-199a-5p during osteoblast maturation.

The different mechanisms of MSC osteoblast differentiation at early and late stage indicated the importance of pre-treating cells before application of hMSC for tissue engineering and regenerative medicine. However, the mechanism of hsa-miR-199a-5p on osteogenesis at early stage needs further clarification. Previously it was showed that hsa-miR-199a-5p may target LIF [9], which could maintain MSC undifferentiated and keep its stemness. This observation together with our data suggests that hsa-miR-199a-5p may initiate MSC differentiation by suppressing stemness genes and promote osteoblast maturation by regulating HIF1α-Twist1 pathway.

5. Conclusion

In conclusion, our results show that the hypoxic condition and activity of HIF1a-Twist1 or miR-199a-5p pathway at correct time point is important for osteogenic differentiation of hMSCs and bone regeneration *in vivo*. Importantly, we successfully encapsulated the agomir into the chitosan nanoparticle for transfection of cultured hMSCs and promoting *in vivo* bone regeneration, suggesting that therapeutic approaches targeting HIF1α-Twist1-miR-199a-5p pathway could be meaningful in bone differentiation and regeneration.

Acknowledgments

This work was supported by NSFC grants (81330041, 81125014, 31271041), RGC GRF #475910, and Zhejiang Provincial Natural Science Foundation of China (LR14H060001).

Appendix A. Supplementary data

Supplementary data related to this article can be found at http://dx.doi.org/10.1016/j.biomaterials.2015.02.071.

References

[1] Colnot C. Cell sources for bone tissue engineering: insights from basic science. Tissue Eng Part B Rev 2011;17:449–57.
[2] Levi B, Longaker MT. Concise review: adipose-derived stromal cells for skeletal regenerative medicine. Stem Cells 2011;29:576–82.
[3] Lewandowska-Szumiel M, Wojtowicz J. Bone tissue engineering – a field for new medicinal products? Curr Pharm Biotechnol 2011;12:1850–9.
[4] Meijer GJ, de Bruijn JD, Koole R, van Blitterswijk CA. Cell-based bone tissue engineering. PLoS Med 2007;4:e9.
[5] Zhang ZY, Teoh SH, Hui JH, Fisk NM, Choolani M, Chan JK. The potential of human fetal mesenchymal stem cells for off-the-shelf bone tissue engineering application. Biomaterials 2011;33:2656–72.
[6] Boyette LB, Creasey OA, Guzik L, Lozito T, Tuan RS. Human bone marrow-derived mesenchymal stem cells display enhanced clonogenicity but impaired differentiation with hypoxic preconditioning. Stem Cells Transl Med 2014;3:241–54.
[7] Preda MB, Ronningen T, Burlacu A, Simionescu M, Moskaug JO, Valen G. Remote transplantation of mesenchymal stem cells protects the heart against ischemia-reperfusion injury. Stem Cells 2014;32:2123–34.
[8] Furtado MB, Costa MW, Pranoto EA, Salimova E, Pinto AR, Lam NT, et al. Cardiogenic genes expressed in cardiac fibroblasts contribute to heart development and repair. Circ Res 2014;114:1422–34.
[9] Oskowitz AZ, Lu J, Penfornis P, Ylostalo J, McBride J, Flemington EK, et al. Human multipotent stromal cells from bone marrow and microRNA: regulation of differentiation and leukemia inhibitory factor expression. Proc Natl Acad Sci U S A 2008;105:18372–7.
[10] Suomi S, Taipaleenmaki H, Seppanen A, Ripatti T, Vaananen K, Hentunen T, et al. MicroRNAs regulate osteogenesis and chondrogenesis of mouse bone marrow stromal cells. Gene Regul Syst Bio 2008;2:177–91.
[11] Lin EA, Kong L, Bai XH, Luan Y, Liu CJ. miR-199a, a bone morphogenic protein 2-responsive MicroRNA, regulates chondrogenesis via direct targeting to Smad1. J Biol Chem 2009;284:11326–35.
[12] Watanabe T, Sato T, Amano T, Kawamura Y, Kawamura N, Kawaguchi H, et al. Dnm3os, a non-coding RNA, is required for normal growth and skeletal development in mice. Dev Dyn 2008;237:3738–48.
[13] Laine SK, Alm JJ, Virtanen SP, Aro HT, Laitala-Leinonen TK. MicroRNAs miR-96, miR-124, and miR-199a regulate gene expression in human bone marrow-derived mesenchymal stem cells. J Cell Biochem 2012;113:2687–95.
[14] Nelson CE, Kim AJ, Adolph EJ, Gupta MK, Yu F, Hocking KM, et al. Tunable delivery of siRNA from a biodegradable scaffold to promote angiogenesis in vivo. Adv Mater 2014;26. 607-14, 506.
[15] Ghosh R, Singh LC, Shohet JM, Gunaratne PH. A gold nanoparticle platform for the delivery of functional microRNAs into cancer cells. Biomaterials 2013;34:807–16.
[16] Sohn YD, Somasuntharam I, Che PL, Jayswal R, Murthy N, Davis ME, et al. Induction of pluripotency in bone marrow mononuclear cells via polyketal nanoparticle-mediated delivery of mature microRNAs. Biomaterials 2013;34:4235–41.
[17] Zhou Y, Zhang L, Zhao W, Wu Y, Zhu C, Yang Y. Nanoparticle-mediated delivery of TGF-beta1 miRNA plasmid for preventing flexor tendon adhesion formation. Biomaterials 2013;34:8269–78.
[18] Yin H, Kanasty RL, Eltoukhy AA, Vegas AJ, Dorkin JR, Anderson DG. Non-viral vectors for gene-based therapy. Nat Rev Genet 2014;15:541–55.
[19] Burnett JC, Rossi JJ. RNA-based therapeutics: current progress and future prospects. Chem Biol 2012;19:60–71.
[20] Sun NF, Liu ZA, Huang WB, Tian AL, Hu SY. The research of nanoparticles as gene vector for tumor gene therapy. Crit Rev Oncol Hematol 2014;89:352–7.
[21] Huang PI, Lo WL, Cherng JY, Chien Y, Chiou GY, Chiou SH. Non-viral delivery of RNA interference targeting cancer cells in cancer gene therapy. Curr Gene Ther 2012;12:275–84.
[22] Ragelle H, Vandermeulen G, Preat V. Chitosan-based siRNA delivery systems. J Control Release 2013;172:207–18.
[23] Almalik A, Day PJ, Tirelli N. HA-coated chitosan nanoparticles for CD44-mediated nucleic acid delivery. Macromol Biosci 2013;13:1671–80.
[24] Gu S, Chan WY. Flexible and versatile as a Chameleon-Sophisticated functions of microRNA-199a. Int J Mol Sci 2012;13:8449–66.
[25] Mizuno S, Bogaard HJ, Gomez-Arroyo J, Alhussaini A, Kraskauskas D, Cool CD, et al. MicroRNA-199a-5p is associated with hypoxia-inducible factor-1alpha expression in lungs from patients with COPD. Chest 2012;142:663–72.
[26] Kang SG, Lee WH, Lee YH, Lee YS, Kim SG. Hypoxia-inducible factor-1alpha inhibition by a pyrrolopyrazine metabolite of oltipraz as a consequence of microRNAs 199a-5p and 20a induction. Carcinogenesis 2012;33:661–9.
[27] Gonsalves CS, Kalra VK. Hypoxia-mediated expression of 5-lipoxygenase-activating protein involves HIF-1alpha and NF-kappaB and microRNAs 135a and 199a-5p. J Immunol 2010;184:3878–88.
[28] Campard D, Lysy PA, Najimi M, Sokal EM. Native umbilical cord matrix stem cells express hepatic markers and differentiate into hepatocyte-like cells. Gastroenterology 2008;134:833–48.
[29] Pittenger MF, Mackay AM, Beck SC, Jaiswal RK, Douglas R, Mosca JD, et al. Multilineage potential of adult human mesenchymal stem cells. Science 1999;284:143–7.
[30] Katas H, Alpar HO. Development and characterisation of chitosan nanoparticles for siRNA delivery. J Control Release 2006;115:216–25.
[31] Nagao M, Feinstein TN, Ezura Y, Hayata T, Notomi T, Saita Y, et al. Sympathetic control of bone mass regulated by osteopontin. Proc Natl Acad Sci U S A 2011;108:17767–72.
[32] Maeno T, Moriishi T, Yoshida CA, Komori H, Kanatani N, Izumi S, et al. Early onset of Runx2 expression caused craniosynostosis, ectopic bone formation, and limb defects. Bone 2011;49:673–82.
[33] Eskildsen T, Taipaleenmaki H, Stenvang J, Abdallah BM, Ditzel N, Nossent AY, et al. MicroRNA-138 regulates osteogenic differentiation of human stromal (mesenchymal) stem cells in vivo. Proc Natl Acad Sci U S A 2011;108:6139–44.
[34] Yang DC, Yang MH, Tsai CC, Huang TF, Chen YH, Hung SC. Hypoxia inhibits osteogenesis in human mesenchymal stem cells through direct regulation of RUNX2 by TWIST. PLoS One 2011;6:e23965.
[35] Wan C, Gilbert SR, Wang Y, Cao X, Shen X, Ramaswamy G, et al. Activation of the hypoxia-inducible factor-1alpha pathway accelerates bone regeneration. Proc Natl Acad Sci U S A 2008;105:686–91.
[36] Marie PJ, Fromigue O. Osteogenic differentiation of human marrow-derived mesenchymal stem cells. Regen Med 2006;1:539–48.
[37] Liu J, Liu T, Zheng Y, Zhao Z, Liu Y, Cheng H, et al. Early responses of osteoblast-like cells to different mechanical signals through various signaling pathways. Biochem Biophys Res Commun 2006;348:1167–73.
[38] Komori T. Regulation of bone development and extracellular matrix protein genes by RUNX2. Cell Tissue Res 2010;339:189–95.
[39] Lee YB, Bantounas I, Lee DY, Phylactou L, Caldwell MA, Uney JB. Twist-1 regulates the miR-199a/214 cluster during development. Nucleic Acids Res 2009;37:123–8.
[40] Tsai CC, Chen YJ, Yew TL, Chen LL, Wang JY, Chiu CH, et al. Hypoxia inhibits senescence and maintains mesenchymal stem cell properties through down-regulation of E2A-p21 by HIF-TWIST. Blood 2011;117:459–69.
[41] Rane S, He M, Sayed D, Vashistha H, Malhotra A, Sadoshima J, et al. Down-regulation of miR-199a derepresses hypoxia-inducible factor-1alpha and Sirtuin 1 and recapitulates hypoxia preconditioning in cardiac myocytes. Circ Res 2009;104:879–86.
[42] Bialek P, Kern B, Yang X, Schrock M, Sosic D, Hong N, et al. A twist code determines the onset of osteoblast differentiation. Dev Cell 2004;6:423–35.
[43] Li Y, Lu Y, Maciejewska I, Galler KM, Cavender A, D'Souza RN. TWIST1 promotes the odontoblast-like differentiation of dental stem cells. Adv Dent Res 2011;23:280–4.
[44] Goodnough LH, Chang AT, Treloar C, Yang J, Scacheri PC, Atit RP. Twist1 mediates repression of chondrogenesis by beta-catenin to promote cranial bone progenitor specification. Development 2012;139:4428–38.
[45] Gradus B, Hornstein E. Role of microRNA in Skeleton Development. Bone Dev 2010;6:81–91.